Development 138, 577-587 (2011) doi:10.1242/dev.053132

Coordination of mitosis and morphogenesis: role of a prolonged G2 phase during chordate neurulation

Yosuke Ogura[1], Asako Sakaue-Sawano[2,3], Masashi Nakagawa[4], Nori Satoh[5], Atsushi Miyawaki[2,3] and Yasunori Sasakura[1,*]

SUMMARY

Chordates undergo a characteristic morphogenetic process during neurulation to form a dorsal hollow neural tube. Neurulation begins with the formation of the neural plate and ends when the left epidermis and right epidermis overlying the neural tube fuse to close the neural fold. During these processes, mitosis and the various morphogenetic movements need to be coordinated. In this study, we investigated the epidermal cell cycle in *Ciona intestinalis* embryos in vivo using a fluorescent ubiquitination-based cell cycle indicator (Fucci). Epidermal cells of *Ciona* undergo 11 divisions as the embryos progress from fertilization to the tadpole larval stage. We detected a long G2 phase between the tenth and eleventh cell divisions, during which fusion of the left and right epidermis occurred. Characteristic cell shape change and actin filament regulation were observed during the G2 phase. CDC25 is probably a key regulator of the cell cycle progression of epidermal cells. Artificially shortening this G2 phase by overexpressing CDC25 caused precocious cell division before or during neural tube closure, thereby disrupting the characteristic morphogenetic movement. Delaying the precocious cell division by prolonging the S phase with aphidicolin ameliorated the effects of CDC25. These results suggest that the long interphase during the eleventh epidermal cell cycle is required for neurulation.

KEY WORDS: Cell cycle, Morphogenetic movement, Chordate, Neurulation, Epidermis, *Ciona intestinalis*

INTRODUCTION

At the initial stages of animal embryogenesis, blastomeres undergo rapid and synchronous cell division called cleavage, which is characterized by very short gap (G1 and G2) phases. When embryogenesis proceeds, longer G1 and/or G2 phases are introduced, and from then on, blastomeres undergo the conventional cell cycle (Kipreos, 2005; Philpott and Yew, 2008). This transition in cell cycle composition is thought to be an adjustment that allows morphogenetic movement to occur (Duncan and Su, 2004). Studies in the protostome *Drosophila melanogaster* have shown that the G2 phase is added at the 14th cell cycle from fertilization (Grosshans and Wieschaus, 2000; Nabel-Rosen et al., 2005). The addition of the G2 phase is necessary for proper morphogenetic movement, as disruption of the G2 phase insertion in *tribbles* mutants leads to gastrulation defects (Mata et al., 2000). A similar phenomenon has been observed in the vertebrate *Xenopus laevis*, in which cell cycle arrest around the midblastula transition (MBT) is necessary for gastrulation (Murakami et al., 2004) and for the convergent extension of paraxial mesoderm (Leise and Mueller, 2004). These studies suggest the importance of changes in cell cycle composition for morphogenesis in both protostomes and deuterostomes. To understand the mechanisms of morphogenesis, we must determine how morphogenetic movement and the cell cycle are balanced.

[1]Shimoda Marine Research Center, University of Tsukuba, Shimoda, Shizuoka 415-0025, Japan. [2]Laboratory for Cell Function and Dynamics, Advanced Technology Development Group, Brain Science Institute, RIKEN, 2-1 Hirosawa, Wako-city, Saitama 351-0198, Japan. [3]Life Function and Dynamics, ERATO, JST, 2-1 Hirosawa, Wako-city, Saitama 351-0198, Japan.[4]Department of Life Science, Graduate School of Life Science, University of Hyogo, 3-2-1 Kouto, Kamigori, Ako-gun, Hyogo 678-1297, Japan. [5]Marine Genomics Unit, Okinawa Institute of Science and Technology Promotion Corporation, Uruma, Okinawa 904-2234, Japan.

*Author for correspondence (sasakura@kurofune.shimoda.tsukuba.ac.jp)

Accepted 21 November 2010

Neurulation is a key morphogenetic movement of chordate embryos that involves the dorsal hollow neural tube (Gilbert, 2006). Neurulation occurs in two parts, primary neurulation and secondary neurulation. Primary neurulation consists of multiple steps: formation of the neural plate; invagination of the neural plate to form the neural groove; convergent extension of the neural plate cells; and closure of the neural tube by the fusion of the left and right neural folds, including the epidermal layer that overlays the neural tube (Colas and Schoenwolf, 2001). Cellular and molecular mechanisms of neurulation have been analyzed extensively; the invagination of the neural plate occurs by apical constriction mediated by Shroom (Hildebrand and Soriano, 1999) and p190RhoGAP (Brouns et al., 2000), and convergent extension of the neural plate is caused by the planar cell polarity (PCP) pathway (Wallingford, 2006). It has been shown that neurulation cannot be accomplished solely by means of the intrinsic movement of the neural plate: contribution from the surrounding epidermis is required for appropriate neural tube formation. The transcription factor AP-2, which is expressed in the epidermis but not in the neural plate, is necessary for proper neural tube closure (Zhang et al., 1996). It has been suggested that the expansion of the epidermal layer, which can be attributed to changes in cell shape, position and number, produces the pushing force that causes the neural plate to bend (Sausedo et al., 1997). Hence, epidermal cells engage in both cell division and morphogenetic movement during neurulation. However, coordination between the cell cycle and the morphogenetic movement of the epidermal layer has not been fully elucidated in vertebrate neurulation. One limitation is that vertebrate neurula-stage embryos consist of an enormous number of cells, and it is thus difficult to trace the cell cycle in a tissue-specific manner. Another experimental system is needed to overcome this problem.

The ascidian *Ciona intestinalis* is an excellent species in which to observe cell cycle progression during neurulation (Satoh, 2003). Like vertebrate embryos, *Ciona* embryos undergo neurulation to

construct a dorsal hollow neural tube. The manner of *Ciona* neurulation is closely related to primary neurulation in vertebrates (Nicol and Meinertzhagen, 1988a; Nicol and Meinertzhagen, 1988b; Lowery and Sive, 2004). *Ciona* embryos and larvae are semi-transparent, and the number of constituent cells is extraordinarily small. The larva consists of ~2,600 cells, with approximately 800 monolayer epidermal cells (Satoh, 1994). The small cell number is advantageous for observing the cell cycle during neurulation at cellular resolution (Nicol and Meinertzhagen, 1988a; Nicol and Meinertzhagen, 1988b). Cell lineage studies have allowed the observation of cell cycle progression in a specific lineage (Nishida, 1987; Pasini et al., 2006). The lineage tracing experiments have shown that epidermal cells undergo seven divisions before the initiation of gastrulation at the 110-cell stage, and divide four times during gastrulation, neurulation and tailbud formation. The epidermal cells then stop dividing until the hatching of larvae (Pasini et al., 2006).

A fluorescent ubiquitination-based cell cycle indicator (Fucci) was recently developed to trace the cell cycle during development in vivo (Sakaue-Sawano et al., 2008). The Fucci system utilizes fusions of fluorescent proteins and the ubiquitination boxes of two proteins, Geminin and Cdt1. Geminin is accumulated in the S, G2 and M phases and degraded in the late M phase, whereas Cdt1 is accumulated in the G1 phase and degraded during the S, G2 and M phases (Nishitani et al., 2004). Therefore, fluorescence of the Geminin-based indicator corresponds to the S/G2/M phases and the Cdt1-based indicator corresponds to the G1 phase. In this study, we introduced this system into *Ciona* embryos together with time-lapse imaging to observe cell cycle progression during neurulation. We found that a long G2 phase is inserted in the specific cell cycle between the tenth and eleventh divisions of epidermal cells. This cell cycle event coincides with the timing of neural tube closure by means of the fusion of the left and right epidermis. Through genetic and pharmacological analyses we show that the prolongation of the cell cycle is necessary for neural tube closure to occur.

MATERIALS AND METHODS

Constructs

A *Ci-EF1α* promoter (Sasakura et al., 2010) was inserted into the multicloning site of pcDNA3-mAG-hGem(1/110), pcDNA3-mVenus-hGem(1/110), pcDNA3-mKO2-hCdt1(1/100), pcDNA3-mKO2-hCdt1(30/120) or pT2-mKO2-zCdt1(1/170). An RfC1 cassette was inserted into pcDNA3-CiEF1α–mKO2-hCdt1(1/100), pcDNA3-CiEF1α–mKO2-hCdt1(30/120) and pT2-CiEF1α–mKO2-zCdt1(1/170). *Ci-EF1α*–mAG-hGem(1/110) was inserted by the Gateway system (Invitrogen). *gap43-egfp* of pSP72-pFOG::B1-GAP43-GFP-B2 (Roure et al., 2007) was inserted into pSP-eGFP, then *egfp* was replaced by *ecfp* to create pSPGAP43C. A *Ci-Epi1* promoter was inserted into pSPGAP43C to create pSPCiEpi1GAP43C. A CAAX box (Fukano et al., 2007) was subcloned into pSPKaede (Hozumi et al., 2010), pSP-Venus and pSP-mCherry to create pSP-KCAAX, pSPVCAAX and pSPmCheCAAX, respectively. A *Ci-Epi1* promoter was inserted into pSPKCAAX to create pSPCiEpi1KCAAX. A *Bam*HI fragment of *Ci-ETR* promoter was inserted into pSPmCheCAAX to create pSPCiETRmCheCAAX. The *egfp* cDNA of pSP-eGFP was replaced by a cDNA of *Ci-cdc25*, then a *Ci-Epi1* promoter was inserted to create pSPCiEpi1Cicdc25. *CiEpi1-gap43-ecfp*, *CiEpi1-KCAAX*, *CiEpi1-VCAAX*, and *CiEpi1-mCheCAAX* were subcloned into pSPCiEpi1Cicdc25 to create pSPCiEpi1Cicdc25CiEpi1GAP43C, pSPCiEpi1Cicdc25CiEpi1KCAAX, pSPCiEpi1Cicdc25CiEpi1VCAAX and pSPCiEpi1Cicdc25CiEpi1mCheCAAX, respectively. The *egfp* cDNA of pSP-eGFP was replaced by a histone 2B ORF (Roure et al., 2007) fused with mCherry, and then a *Ci-Epi1* promoter was inserted to create pSPCiEpi1H2BmCherry. Fucci constructs and H2BmCherry cassettes were inserted into pBS-HTB (Akanuma et al., 2002). mRNA was synthesized with the Megascript T3 (Ambion), cap structure analog (New England Biolabs), and poly(A) tailing kit (Ambion).

Time-lapse imaging using wide-field microscopy

The vectors shown in Fig. 1A were electroporated into one-cell-stage embryos (Corbo et al., 1997). The embryos were reared at 18°C until imaging. Time-lapse imaging was performed using the AxioImager Z1 wide-field fluorescent microscope system (Carl Zeiss). Imaging was performed in a room maintained at 20°C. We found no significant deviation from the developmental table (Hotta et al., 2007) defined at 18°C until 8.5 hours post fertilization (hpf). pSPCiEpi1GAP43C and pSPCiEpi1CiCdc25CiEpi1GAP43C (linearized with *Xho*I) were microinjected into unfertilized eggs together with mVenus-hGem(1/110) mRNA. At 6.0 hpf, the embryos were mounted on a glass-based dish, and time-lapse imaging was performed. The recording interval was 5 minutes. In the aphidicolin administration experiment, imaging was halted at 6 hours 55 minutes, aphidicolin was added at the concentration of 2 μg/ml, and imaging was restarted from 7.0 hpf.

Time-lapse imaging using confocal laser scanning microscopy

To observe the global cell cycle progression pattern, we microinjected mAG-hGem(1/110) and mKO2-hCdt1(1/100) mRNA into unfertilized eggs. For epidermal cell tracking experiments, mRNA of H2BmCherry was microinjected with mRNA of mAG-hGem(1/110). At 5-6 hpf, the embryos were mounted on a glass-based dish, and time-lapse 3D imaging was performed using an FV10i confocal microscope (Olympus) at 20°C. The recording interval was either 5 minutes or 10 minutes. At each time point, *z*-stack images were generated in the Fluoview viewer (Olympus). To observe cell shape change during the neural tube closure, pSPCiEpi1KCAAX or pSPCiEpi1Cicdc25CiEpi1KCAAX was electroporated into one-cell-stage embryos. At 5-6 hpf, the embryos were mounted on a glass-based dish and 10 μM FM4-64 (Molecular Probes) was added. Embryos were treated with 100 μM Y-27632 from 6.0 hpf.

Whole-mount in situ hybridization

Whole-mount in situ hybridization was performed essentially according to Yasuo and Satoh (Yasuo and Satoh, 1994). pSPCicdc25 was digested with *Sal*I and *Eco*RI, and this partial cDNA fragment of *Ci-cdc25* was inserted into the *Sal*I and *Eco*RI sites of pBluescript SKII+. This vector was used as a template to synthesize digoxigenin-labeled probes for in situ hybridization. Probes were washed at 55°C and the final washing step was carried out using 30 mM NaCl, 3 mM sodium citrate, 0.1 % Tween 20.

Incorporation of EdU

The embryos were treated with 10 μM 5-ethynyl-2′-deoxyuridine (EdU) at 6.5 hpf, 7.0 hpf or 7.5 hpf for 30 minutes at 18°C. After fixation with 5% formaldehyde in sea-water, EdU incorporation was detected with a Click-iT EdU Alexa Fluor Imaging Kit (Invitrogen).

Immunostaining and phalloidin staining

mVenus-hGem(1/110) was immunostained with anti-GFP antibody (1:1000; Nacalai Tesque) and Alexa-488-conjugated anti-rabbit antibody (Invitrogen) for observation of EdU incorporation in Fucci-expressing embryos. To detect Phospho-histone H3 (PH3), pSPCiEpiIH2BmCherry was introduced into embryos, which were fixed at 7.75 hpf. PH3 was stained with anti-PH3 Ser10 antibody (1:100) (Tarallo and Sordino, 2004) and Alexa-488 conjugated anti-rabbit antibody. Embryos were stained with Alexa-488-conjugated phalloidin (Invitrogen) to detect F-actin.

RESULTS

Application of live-imaging probes to monitor cell cycle progression in *Ciona intestinalis* embryos

Several derivatives of Fucci probes have been created that are optimized for vertebrates (Sakaue-Sawano et al., 2008; Sugiyama et al., 2009). We tested whether these Fucci probes could monitor cell cycle progression in *Ciona*. For the Geminin-based Fucci, we tested mAG-hGem(1/110) and mVenus-hGem(1/110), which are

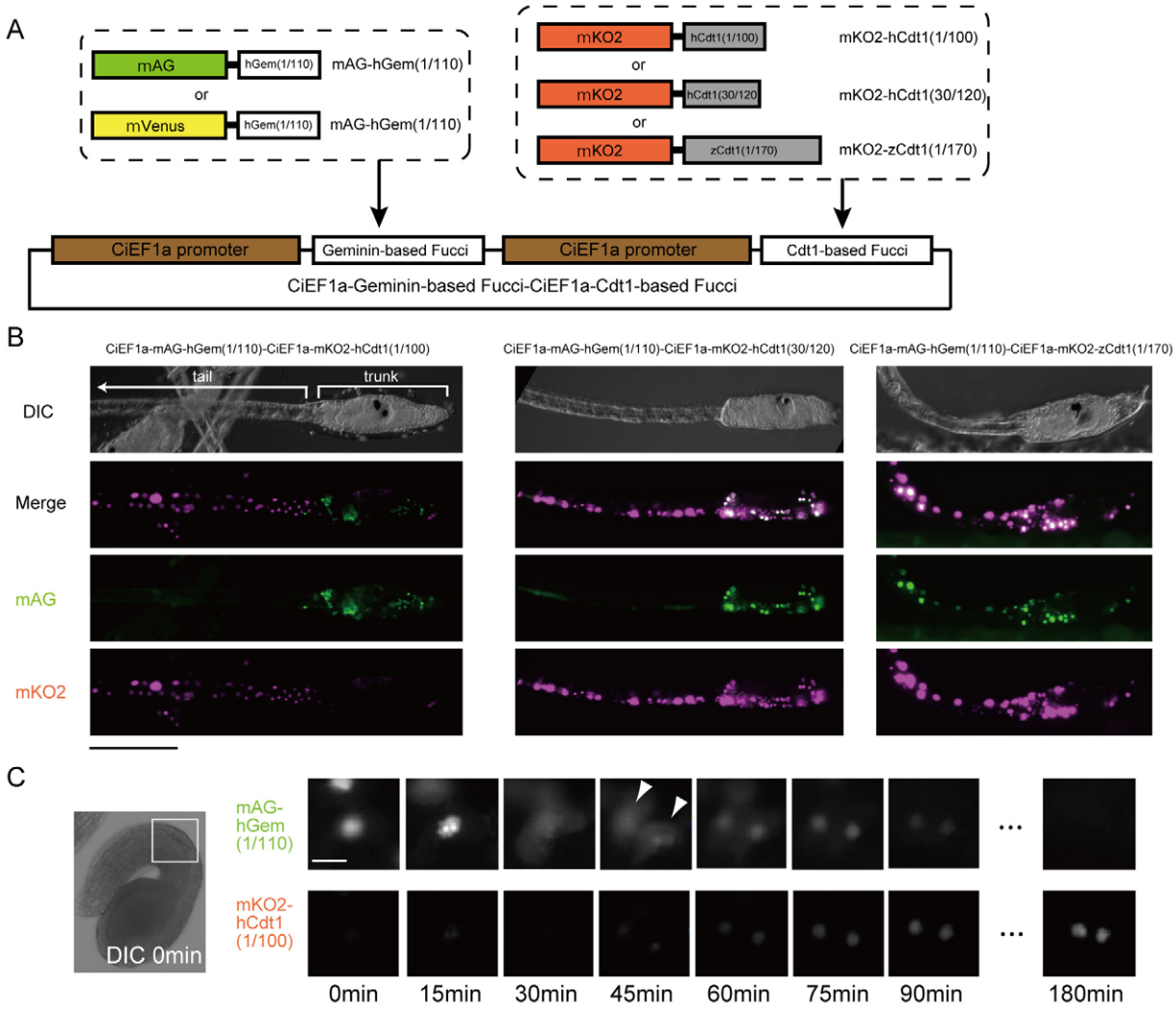

Fig. 1. Selection of Fucci probes that can monitor cell cycle progression in *Ciona*. (**A**) Schematic diagrams of DNA vectors used for the test of Fucci. DNAs encoding these Fucci probes were fused with *Ci-EF1α* promoters (brown boxes). Geminin-based constructs and Cdt1-based constructs are included in the same vector. (**B**) Expression pattern of three Cdt1-based Fucci probes (mKO2, magenta) with mAG-hGem(1/110) (mAG, green) at the larval stage. Scale bar: 50 μm. (**C**) Time-lapse imaging of the fluorescence of mAG-hGem(1/110) and mKO2-hCdt1(1/100) in an epidermal cell. On the left is the DIC image of the tailbud embryo at the start of imaging (0 minutes). The box indicates the region shown in the other images. To the right, the top row shows expression of mAG-hGem(1/110) and the bottom row shows expression of mKO2-hCdt1(1/100) at the times indicated. The traced cell divided at 45 minutes after imaging began; the sister cells are shown by arrowheads. Scale bar: 5 μm. DIC, differential interference contrast.

fusions of a part of human Geminin (amino acids 1-110) with monomeric Azami Green (mAG) and monomeric Venus-YFP (mVenus), respectively. The Geminin-based Fucci probes emit green fluorescence. For Cdt1-based Fucci, there are two different human Cdt1 (hCdt1)-based Fucci probes: one includes amino acids 1-100 [hCdt1(1/100)] and the other includes amino acids 30-120 [hCdt1(30/120)]. We also tested a zebrafish Cdt1 (zCdt1)-based probe that includes amino acids 1-170. DNAs encoding these partial Cdt1 proteins were fused with cDNAs of monomeric Kusabira Orange 2 (mKO2), resulting in emission of orange fluorescence upon expression.

Expression of these Fucci probes was driven in the *Ciona* embryos and larvae with a ubiquitous promoter of *Ci-EF1α* (Fig. 1A) (Sasakura et al., 2010). At the larval stage, most cells in the tail stop cell cycle progression, and therefore cells in the S/G2/M phases are restricted to the trunk region (Nakayama et al., 2005). Accordingly, the fluorescence of mAG-hGem(1/110) and mVenus-hGem(1/110) was observed exclusively in the trunk (Fig. 1B, left), suggesting that these Fucci probes successfully monitor the S/G2/M phases in *Ciona* embryos. When mKO2-hCdt1(1/100) and mAG-hGem(1/110) were simultaneously expressed, the orange fluorescence rarely overlapped with the green fluorescence, suggesting that mKO2-hCdt1(1/100) is degraded at the S/G2/M phases. Almost all cells in the tail showed orange fluorescence exclusively, suggesting that their cell cycle is arrested at the G1/G0 phase. When mKO2-hCdt1(30/120) and mAG-hGem(1/110) were simultaneously expressed, the green fluorescence in the trunk always overlapped with the orange fluorescence (Fig. 1B, middle), suggesting that mKO2-hCdt1(30/120) is not degraded in the S/G2/M phases. Because cells at the tail region showed mKO2-hCdt1(30/120) fluorescence exclusively, cell cycle progression was not strongly affected by mKO2-hCdt1(30/120). When mKO2-

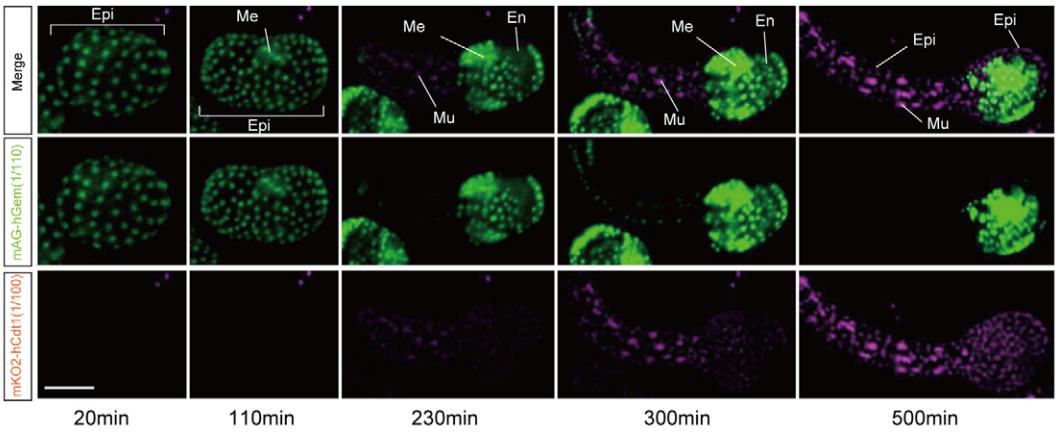

Fig. 2. Time-lapse imaging of a *Ciona* embryo into which mAG-hGem(1/110) and mKO2-hCdt1(1/100) mRNA were introduced. Expression of mAG-hGem(1/110) is shown in green and that of mKO2-hCdt1(1/100) in magenta. The time after the start of imaging is shown at the bottom. Scale bar: 50 μm. Me, mesenchyme; En, endoderm; Epi, epidermis; Mu, muscle.

zCdt1(1/170) was expressed together with mAG-hGem(1/110), the cells in the tail expressed both green and orange fluorescence (Fig. 1B, right), suggesting that mKO2-zCdt1(1/170) inhibits normal cell cycle progression. Our results indicate that mAG-hGem(1/110), mVenus-hGem(1/110) and mKO2-hCdt1(1/100) can be used to monitor cell cycle progression during *Ciona* embryogenesis.

To confirm this, we imaged mAG-hGem(1/110) and mKO2-hCdt1(1/100) fluorescence at single-cell resolution. After these two Fucci probes were simultaneously expressed in the epidermal cells of a tailbud embryo, epidermal cells with green nuclei were time-lapse imaged (Fig. 1C). The intense mAG-hGem(1/110) fluorescence in the nucleus was redistributed throughout the cells, probably upon nuclear envelope breakdown (Fig. 1C, 30 minutes). The dispersion of the Geminin-based Fucci signal can be used to determine the timing of the beginning of prometaphase. The cytokinesis of these cells that follows the prometaphase was observed in the form of dispersed mAG-hGem(1/110) fluorescence making an outline of the cell shape (Fig. 1C, 45 minutes). After cell division was completed, mAG-hGem(1/110) fluorescence was again accumulated in the nuclei (Fig. 1C, 60-75 minutes) and then disappeared after 30 minutes. mKO2-hCdt1(1/100) started to accumulate in the nuclei soon after cell division was finished (Fig. 1C, 60-90 minutes), and the timing was complementary to that of mAG-hGem(1/110). We concluded that mAG-hGem(1/110), mVenus-hGem(1/110) and mKO2-hCdt1(1/100) can be used to observe cell cycle progression in *Ciona* embryos and larvae.

Cell cycle progression of epidermal cells during neurulation

By using mAG-hGem(1/110) and mKO2-hCdt1(1/100), we monitored cell cycle progression in the epidermis at whole-embryo resolution (Figs 2 and 3). In vitro-synthesized mRNAs of the two Fucci probes were simultaneously introduced into unfertilized eggs by microinjection, and observation was begun after fertilization. This method reduces the mosaicism of the expression levels of probes among cells in comparison with DNA electroporation. The eighth mitosis of the epidermal cells was completed by 5.0 hpf and could not be followed by the accumulation of mAG-hGem(1/110) due to a lack of detectable fluorescence. The accumulation of mAG-hGem(1/110) was observed at ~5.0 hpf (see Movie 1 in the supplementary material), after the eighth mitosis. The ninth mitosis occurred at 5.5-6.0 hpf (Fig. 2, Fig. 3A,E; see Movie 1 in the supplementary material). The b-line (posterior) epidermal cells divided ~5 minutes faster than the a-line (anterior) cells, as was described previously (Nishida 2005). After this ninth division, the accumulation of mKO2-hCdt1(1/100) was not detected and mAG-hGem(1/110) accumulation was soon restarted (Fig. 2; see Movie 1 in the supplementary material), suggesting that there is only a short G1 phase and that cells enter the S/G2 phase soon after the ninth division. The tenth mitosis occurred at 6.5-7.0 hpf (Fig. 2, Fig. 3B,E; see Movie 1 in the supplementary material). We found that the timing of this division differed along the anterior-posterior (A-P) axis of the embryo. Posterior cells tended to start dividing earlier than anterior cells (Fig. 3B). After this tenth division, the accumulation of mKO2-hCdt1(1/100) was not detected, and mAG-hGem(1/110) accumulation was soon restarted (Fig. 2; see Movie 1 in the supplementary material). The fluorescence of mAG-hGem(1/110) showed that the eleventh division occurred at ~8.0-9.0 hpf (Fig. 2, Fig. 3C,E; see Movie 1 in the supplementary material). At the time of the eleventh cell division, epidermal cells can be subdivided into four groups with different mitotic domains: cells around the ventral midline (MD1) and dorsal midline (MD2) and cells on the trunk lateral side (MD3a) and tail lateral side (MD3b) (Fig. 3C,D). In this study, the term ‘mitotic domain’ (Foe and Odell, 1989) indicates a group of cells consisting of a single mitotic wave and sharing the timing of the entrance into the prometaphase. The eleventh mitosis started in the following order: MD1, MD2, MD3 (Fig. 3C). In MD1, MD2 and MD3a, posterior cells started mitosis earlier and the mitotic wave moved toward the anterior (Fig. 3D). Cells at MD3b showed a different pattern: mitosis started from both the anterior and posterior sides, and cells in the middle part underwent mitosis later (Fig. 3D). After the eleventh division, the epidermal cells started to accumulate mKO2-hCdt1(1/100) (Fig. 2; see Movie 1 in the supplementary material).

The intervals between the prometaphases of the tenth and eleventh cell divisions were an average of 36-47 minutes longer than those between the ninth and tenth divisions for cells of each mitotic domain, suggesting that the eleventh cell cycle is longer than the tenth cell cycle (Table 1). Because mAG-hGem(1/110) was accumulated in the nuclei at the early phase of the eleventh cell cycle (namely between the tenth and eleventh divisions) and no accumulation of mKO2-hCdt1(1/100) was detected, the longer interval in this period is thought to be due to the long S phase and/or G2 phase. EdU was incorporated around this cell cycle to determine

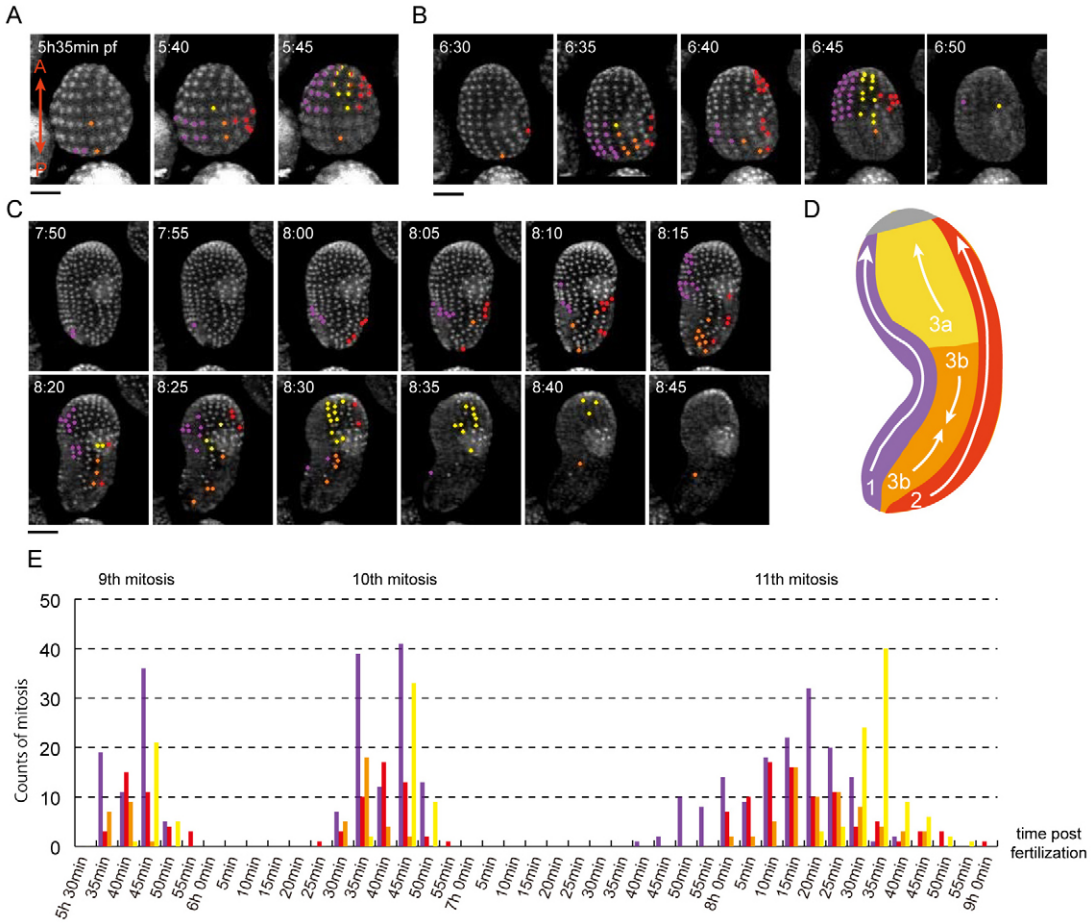

Fig. 3. Mitotic timing of epidermal cells during neurulation. (**A-C**) mAG-hGem(1/110) mRNA-introduced *Ciona* embryos were subjected to time-lapse imaging at 5 minute intervals. Nuclei of the cells that entered the prometaphase in the next 5 minute interval were marked with dots. The colors of the dots correspond to the mitotic domains shown in D. An embryo at the center was viewed from the lateral side. The A-P axis of the embryo is indicated by a double-headed arrow in A. Timing of the ninth (A), tenth (B) and eleventh (C) divisions are shown. (**D**) A schematic diagram of four mitotic domains of the epidermal cells at the tailbud stage. The patterns of progression of mitosis in each mitotic domain are shown by arrows. (**E**) Quantification of the timing at which epidermal cells entered the prometaphase of the ninth, tenth and eleventh cell division. The colors of the bars correspond to the mitotic domains in D. Scale bars: 50 μm.

the timing of the S phase at the eleventh cell cycle. When embryos were treated with EdU at 6.5-7.0 hpf, incorporation of EdU was not observed in the epidermal cells, whereas the neural plate cells showed strong EdU incorporation at this stage (Fig. 4A, left). Because epidermal cells enter the prometaphase of the tenth division at 6.5-7.0 hpf (Fig. 3E), these cells are in the M phase in most of this time window. We cannot exclude the possibility that there is a G1 phase that is too short to detect with Fucci. At 7.0-7.5 hpf, strong EdU incorporation was observed in the epidermal cells (Fig. 4A, middle), suggesting that they were in the S phase. At 7.5-8.0 hpf, incorporation of EdU was again lost in the epidermal cells (Fig. 4A, right). Therefore, the S phase at the eleventh cell cycle occurs within 30 minutes at 7.0-7.5 hpf. Because epidermal cells start to enter the M phase at 8.0 hpf, they are arrested for at least 30 minutes in the G2 phase of this cell cycle. To confirm that epidermal cells are in the G2 phase at 7.5-8.0 hpf, EdU incorporation was performed using embryos in which mVenus-hGem(1/110) was expressed in this time window. Epidermal cells showed accumulation of mVenus-hGem(1/110) in the nuclei, the hallmark of S/G2 phases, whereas no EdU incorporation was detected (Fig. 4B), suggesting that epidermal cells were in the G2 phase.

Time-lapse imaging revealed that closure of the neural tube by the fusing of the left and right epidermis occurred during this long G2 phase (Fig. 4C). Fusion of the epidermis started in the

Table 1. Comparison of the length of the intervals among the ninth, tenth and eleventh cell divisions

	Interval between the prometaphases of the ninth and tenth cell divisions* (minutes)					Interval between the prometaphases of the tenth and eleventh cell divisions* (minutes)								
Mitotic domain	50	55	60	65	Average	80	85	90	95	100	105	110	115	Average
MD1	0	4	8	4	60	0	1	3	7	2	2	1	0	96.3
MD2	4	6	2	2	55.7	1	0	5	2	3	0	3	0	96.4
MD3b	4	6	2	2	55.7	0	2	1	2	4	3	1	1	99.3
MD3a	0	2	20	4	60.4	0	0	0	0	0	13	12	1	107.7

*Number of cells with the corresponding interval length is shown.

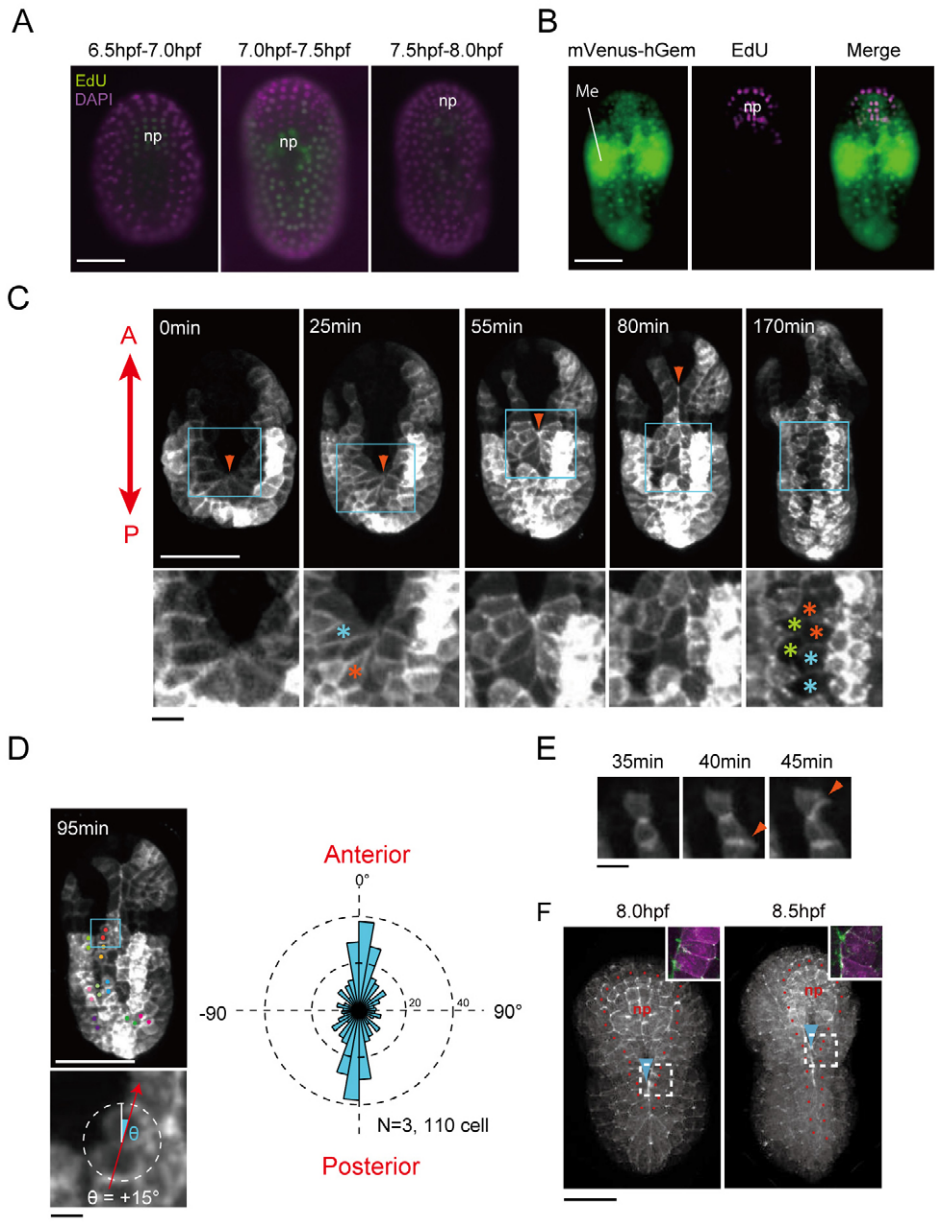

Fig. 4. Fusion of the epidermis during neural tube closure occurs at the G2 phase of the eleventh cell cycle. (**A**) The S phase of the eleventh epidermal cell cycle is ~7.0-7.5 hours post fertilization (hpf). *Ciona* embryos were treated with 5-ethynyl-2′-deoxyuridine (EdU) for 30 minutes at 6.5-7.0, 7.0-7.5 and 7.5-8.0 hpf. Green, incorporation of EdU; magenta, DAPI. Embryos were viewed from the dorsal side. Epidermal cells and neural plate (np) cells showed incorporation of EdU at 7.0-7.5 hpf and 6.5-7.0 hpf, respectively. Scale bar: 50 μm. (**B**) EdU incorporation at 7.5-8.0 hpf in embryos in which mVenus-hGem(1/110) was expressed. Green, mVenus-hGem(1/110); magenta, EdU. Epidermal cells did not incorporate EdU, whereas cells in the neural lineage (np) did. Me, mesenchyme. Scale bar: 50 μm. (**C**) Cell shape changes of epidermal cells during neural tube closure, as revealed by the fluorescence of Kaede-CAAX fusion driven by the *Ci-Epi1* promoter. The top row shows the entire embryo, the bottom row shows a magnified view of the area indicated by the squares in the top row. At 25 minutes, the posterior cells of the dorsal epidermis elongated towards the anterior (red asterisk), and the cells at the lateral side elongated laterally (blue asterisk). These cells made contact at the focus (arrowhead). At 55 minutes, the neural tube of the tail was closed. The cellular focus at the zippering origin moved towards the anterior (arrowhead). At 80 minutes, half of the trunk midline was closed. The eleventh cell division of three cells was tracked (170 minutes) and their daughter cells are marked with asterisks of the same color. Scale bars: 50 and 10 μm for the upper and lower columns, respectively. (**D**) Epidermal cells tend to divide parallel to the A-P axis at the eleventh division. On the left is an example of measurement of the angle between the division orientation and the A-P axis. Sister cells are indicated by dots of the same color. A pair of sister cells just after the eleventh division (red spots in the square in the upper image) is shown at the bottom. The angle (θ) is 15° in this case. On the right is a rose diagram of division orientation of 110 epidermal cells in three embryos. Division angles with respect to the A-P axis are binned from –180° to +180° in bins of 10°. Scale bars: 50 μm for upper image; 10 μm for lower image. (**E**) Filopodia formation of the dorsal midline epidermal cells during neural tube closure. At 40-45 minutes after imaging was started, filopodia (arrowheads) were elongated towards the midline. Scale bar: 10 μm. (**F**) Accumulation of F-actin at the medial end of the dorsal midline epidermis (arrowheads) during neural tube closure, as revealed by phalloidin staining. Red spots indicate the position of the dorsal midline epidermal cells. Insets are magnified colored images of the areas indicated by the squares. Green, phalloidin staining; magenta, plasma membrane of epidermal cells labeled with mCherry-CAAX driven by a promoter of *Ci-Epi1*. Scale bar: 50 μm.

posterior-most region, and the fused plane moved in the anterior direction (see Movie 2 in the supplementary material). Membrane-bound fluorescent proteins were expressed in the epidermal cells to label their plasma membranes, allowing us to observe the cell shape changes of the epidermal cells during the fusion. Epidermal cells that had finished their tenth division were round, and no cell polarity was recognized. At the onset of neural tube closure, epidermal cells at the posterior midline become elongated towards a focus at the dorsal midline (Fig. 4C, arrowheads). These epidermal cells made contact at the focus, which then became the origin of zippering. The left and right lateral epidermal cells moved towards the midline, changed their shape to fill the gap and aligned tightly along the midline to close the furrow (Fig. 4C, 55 minutes). Short filopodia were formed during the cell movement (Fig. 4E), and F-action was accumulated strongly at the medial end of the midline epidermis (Fig. 4F). The movement and alignment of midline epidermal cells were transmitted towards the anterior and the midline was closed as if zipped (Fig. 4C, 80 minutes; see Movie 2 in the supplementary material). After this zippering, the epidermal cells underwent the eleventh division (Fig. 4C, 170 minutes). Epidermal cells of all mitotic domains tended to divide parallel to the A-P axis (Fig. 4C, 170 minutes; Fig. 4D). During neural tube closure, the tail started elongating toward the posterior end of the embryo.

Different timing of *cdc25* expression in epidermal cells along the A-P axis

CDC25 is a conserved cell cycle regulator that promotes both G1/S and G2/M transitions (Boutros et al., 2006). Transcriptional regulation of *cdc25* is crucial for tissue-specific timing of G2/M progression (Edgar et al., 1994; Lehman et al., 1999). If *Ciona cdc25* is responsible for the regulation of epidermal cell G2/M progression, this gene might be expressed at different times along the A-P axis of the embryo. To examine this possibility, we investigated the expression profile of a *cdc25* homolog of *Ciona intestinalis* (*Ci-cdc25*) by whole-mount in situ hybridization (Kawashima et al., 2003). Expression of *Ci-cdc25* was observed in all of the epidermal cells in the early gastrula stage at 5.0-5.5 hpf (see Fig. S1A,B in the supplementary material). At 5.5 hpf, strong expression of *Ci-cdc25* was also observed in cells of the neural lineage (see Fig. S1B in the supplementary material). At 6.0 hpf, ~30 minutes before the start of the tenth mitosis, *Ci-cdc25* expression was observed exclusively in the trunk epidermal cells, and the expression was reduced at 6.5 hpf, except for the anterior-most epidermis (see Fig. S1C,D in the supplementary material). At 7.0 hpf, when the epidermal cells had finished the tenth division and entered the S/G2 phase of the eleventh cell cycle, no expression of *Ci-cdc25* was observed in the epidermal cells (see Fig. S1E in the supplementary material). At 7.5 hpf, when the epidermal cells were in the long G2 phase, expression of *Ci-cdc25* at the posterior-most epidermis restarted (see Fig. S1F in the supplementary material). At 8.0 hpf, when the posterior-most epidermal cells started the eleventh mitosis, strong expression of *Ci-cdc25* was observed in the epidermal cells near the posterior pole of the embryo (see Fig. S1G in the supplementary material). At 8.5-9.0 hpf, when the embryos had finished closing the tail neural tube, weak expression of *Ci-cdc25* was detected in all of the tail epidermal cells (see Fig. S1H,I in the supplementary material). These results indicate that the timing of the expression of *Ci-cdc25* was different in the anterior and posterior epidermal cells. This difference is in accordance with the above-mentioned observation that the timing of cell division in the epidermis differs along the A-P axis of the embryo, and that Ci-CDC25 is a candidate regulator of cell cycle progression of embryonic cells, or at least epidermal cells, during *Ciona* embryogenesis.

A long G2 phase at the eleventh cell cycle of epidermal cells is required for neural tube closure

The temporal correlation between the insertion of the long G2 phase at the eleventh cell cycle of epidermal cells and the closure of the neural tube suggests a causal relationship of these two developmental events. We attempted to reduce the period of this long G2 phase by overexpression of *Ci-cdc25* in epidermal cells in order to observe its effects on neural tube closure (Fig. 5A). *Ci-Epi1* is an epidermis-specific gene that starts to be expressed around the neurula stage (Chiba et al., 1998), and we utilized its cis element for overexpression of *Ci-cdc25*. The cell cycle progression of the epidermal cells of *Ci-cdc25*-overexpressing embryos was normal until the tenth division, as was revealed by the fluorescence of mVenus-hGem(1/110) (Fig. 5B). At the eleventh cell division, a clear difference was observed compared with the control embryos. The *Ci-cdc25*-overexpressing embryos started the eleventh division an average of 40 minutes earlier than the controls. Namely, the period of the eleventh cell cycle (between the tenth and eleventh divisions) was shortened to ~50 minutes compared with 90 minutes in normal embryos. Precocious eleventh epidermal cell division in the *Ci-cdc25*-overexpressing embryos was confirmed by immunostaining of phospho-histone H3 (PH3), a marker of cells during mitosis, at 7.75 hpf (see Fig. S2 in the supplementary material). These *Ci-cdc25*-overexpressing embryos failed to close the neural tube (80%, *n*=25; Table 2). When viewed from the cross-section, the nerve cord of the normal embryos formed a clear tube consisting of four rows of neural cells (see Fig. S3 in the supplementary material). By contrast, neural plate cells of *Ci-cdc25*-overexpressing embryos were aligned laterally to maintain 'sheet' morphology (see Fig. S3 in the supplementary material), suggesting that the sheet-to-tube transition of the neural tissue is arrested by shortening the G2 phase. Forty percent of *Ci-cdc25*-overexpressing embryos had a severe phenotype (Table 2); they did not demonstrate neural tube closure in either the tail or trunk regions (Fig. 5B; see Fig. S4A,B in the supplementary material). In these embryos, epidermal cells underwent the eleventh cell division before the initiation of closure. Formation of a clear zippering origin was not observed at the posterior end of the embryos, and movement of the epidermal cells towards the midline did not occur (Fig. 5C; see Movie 3 in the supplementary material). Forty percent of the embryos (Table 2) showed a milder phenotype; their epidermal cells completed neural tube closure at the tail region but not at the trunk region (see Fig. S4C in the supplementary material). The remaining 20% of the embryos completed neural tube closure (*n*=25; Table 2). In these embryos the eleventh division took place just after the closure, although the timing of the division was earlier than in the wild-type controls (see Fig. S4D in the supplementary material). These results suggest that the eleventh cell

Table 2. *Ci-cdc25* overexpression disrupts neural tube closure

Experiment number	Trunk + tail*	Trunk†	Completed‡	Total
1	4	2	3	9
2	2	4	1	7
3	4	4	1	9
Total	10	10	5	25

*Number of embryos with defects in neural tube closure at both trunk and tail.
†Number of embryos with defects in neural tube closure at trunk.
‡Number of embryos with completed neural tube closure.

division of epidermal cells must take place after neural tube closure for this morphogenetic movement to occur. We examined the orientation of the eleventh epidermal cell division in *Ci-cdc25*-overexpressing embryos. The epidermal cells tended to divide parallel to the A-P axis as in the control embryos, suggesting that the induction of a precocious eleventh mitosis by *Ci-cdc25* did not disrupt its orientation (see Fig. S5 in the supplementary material).

The above data suggest that a long G2 phase at the eleventh cell cycle might be necessary for the eleventh division to occur after the completion of neural tube closure. If this is the case, the long interval between the tenth and eleventh cell divisions is not necessarily the G2 phase. To examine this possibility, we treated embryos with aphidicolin, an inhibitor of DNA replication (Ikegami et al., 1978), between the tenth and eleventh divisions of

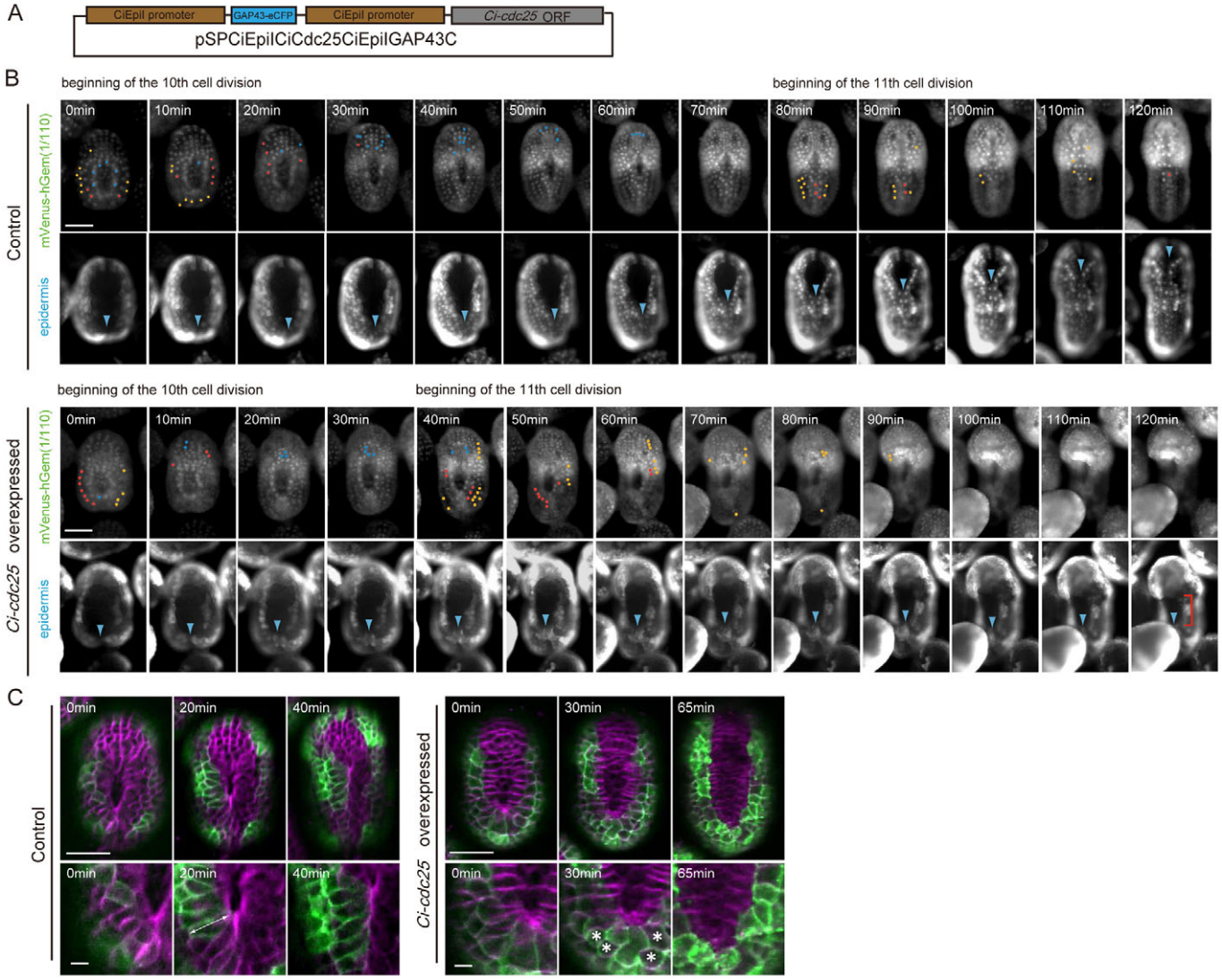

Fig. 5. Overexpression of *Ci-cdc25* in the epidermis disrupts neural tube closure. (**A**) Schematic diagram of a DNA construct used in the *Ci-cdc25* overexpression experiments. *Ci-Epi1* promoters, the *gap43-ecfp* fusion cassette and *Ci-cdc25* cDNA are indicated by brown, blue and gray boxes, respectively. (**B**) Overexpression of *Ci-cdc25* disrupts neural tube closure. Time-lapse images of embryos into which mVenus-hGem(1/110) mRNA and pSPCiEpi1GAP43C (control), or mVenus-hGem(1/110) and pSPCiEpi1Cicdc25CiEpi1GAP43C (*Ci-cdc25* overexpressed), were microinjected. Time-lapse imaging was done at 5 minute intervals and from the dorsal side. In this figure, time-lapse images taken at 10 minute intervals are shown. The beginning of the tenth cell division was set as 0 minutes in each case. Fluorescence of GAP43-CFP fusion (bottom row of each set) shows the area covered by the epidermis. Cells that entered into the prometaphase within the next 10 minute interval were marked with dots (red, dorsal midline epidermal cells; orange, other epidermal cells; blue, neural precursor cells). Note that the eleventh division started 40 minutes after the tenth division in the *Ci-cdc25*-overexpressing embryo, whereas it started at 80 minutes after the tenth division in the control embryo. In the *Ci-cdc25*-overexpressing embryo, neural tube closure did not occur (red bracket). Arrowheads indicate the posterior end of the neural plate. Scale bars: 50 μm. (**C**) Cell shape changes of the epidermal cells during neural tube closure. Single confocal planes of the embryos expressing pSPCiEpi1KCAAX (control) or pSPCiEpi1CiCdc25CiEpi1KCAAX (*Ci-cdc25* overexpressed), dorsal view. Green, plasma membrane of the epidermal cells labeled with Kaede-CAAX; magenta, plasma membrane of all cells stained with FM4-64. In the control embryo, the epidermal cells were elongated towards the midline (20-40 minutes, double-headed arrow). At 40 minutes, the tail epidermal cells moved towards the midline, and the left epidermis and right epidermis were fused. In the *Ci-cdc25*-overexpressing embryo (0-30 minutes), elongation of epidermal cells was not observed and zippering was not initiated, even 65 minutes after the tenth division. Instead, some epidermal cells performed the eleventh division at 30 minutes. Two pairs of daughter cells are indicated by asterisks. Scale bars: 50 and 10 μm for the upper and lower rows within each set, respectively.

Table 3. Aphidicolin treatment prevents defects in neural tube closure in the tail region

Experiment number	Treatment	Normal‡	Defects§
1	*Ci-cdc25*-OE + DMSO*	3	5
	Ci-cdc25-OE + Aph†	8	0
2	*Ci-cdc25*-OE + DMSO	0	6
	Ci-cdc25-OE + Aph	5	3

*_Ci-cdc25_*-overexpressing embryos treated with DMSO from 7.0 hpf.
†_Ci-cdc25_-overexpressing embryos treated with aphidicolin from 7.0 hpf.
‡Number of embryos with normal neural tube closure in the tail region.
§Number of embryos with defects in neural tube closure in the tail region.
Aph, aphidicolin; DMSO, dimethyl sulfoxide; OE, overexpression.

the epidermal cells, and observed its effect on neural tube closure. When embryos were treated with aphidicolin just after the tenth division and before the eleventh division, neural tube closure at the tail region occurred as in the normal embryos (86%, *n*=21). The trunk neural plate did not completely close in the aphidicolin-treated embryos. This could have been because cell cycle progression of the trunk neural plate cells was also affected by aphidicolin. The aphidicolin-treated embryos showed either delayed or no eleventh mitosis of epidermal cells, suggesting that aphidicolin effectively suppressed progression through the S phase of the eleventh cell cycle.

By utilizing aphidicolin, we performed a rescue experiment of the overexpression phenotype of *Ci-cdc25* by arresting cells at the S phase. We noted the occurrence of neural tube closure at the tail. As a result, the *Ci-cdc25*-overexpressing and aphidicolin-treated embryos showed neural tube closure at the tail much more frequently than did *Ci-cdc25*-overexpressing control embryos (Fig. 6 and Table 3), suggesting that induction of a longer interval after the tenth cell division rescued the effect of *Ci-cdc25* overexpression. Fluorescent cross-section showed that a proper tail nerve cord was formed in the *Ci-cdc25*-overexpressing and aphidicolin-treated embryos (see Fig. S3 in the supplementary material). Taken together, these findings suggest that a long interval between the tenth and eleventh cell divisions of epidermal cells is crucial for neural tube closure. The interval is not necessarily the G2 phase, but in normal embryogenesis it occurs as a long G2 phase.

We performed a quantitative analysis to determine how much the shortening of the G2 phase affected the shape change of epidermal cells. As mentioned above, the dorsal midline epidermis was elongated towards the midline during neural tube closure. We measured the length of the cells along the mediolateral axis and the width along the A-P axis to calculate the length/width (L/W) ratio (Table 4); the scores were about 2.21 and 1.69 in the tail and trunk epidermal cells of control embryos, respectively. When *Ci-cdc25* was overexpressed, the L/W ratios were reduced to 1.58 and 1.38, respectively, and aphidicolin administration restored the scores to 1.98 and 1.69, respectively. Therefore, the prolongation of the interphase is necessary for the dorsal midline epidermis to elongate towards the midline. The elongation was also interfered with by treating embryos with Y-27632, an inhibitor of Rho-kinase (ROCK) (Uehata et al., 1997), suggesting that this cell shape change is a result of Rho-mediated ROCK regulation. Y-27632 treatment did not affect the timing or pattern of cell cycle progression (data not shown).

We examined further the effect of the shortening of the G2 phase on F-actin accumulation at the medial end of the dorsal midline epidermis. As a result, F-actin accumulation was significantly decreased in the dorsal midline epidermal cells of *Ci-cdc25*-overexpressing embryos (see Fig. S6 in the supplementary material). F-actin accumulation was ameliorated by prolongation of the S phase with aphidicolin in *Ci-cdc25*-overexpressing embryos (see Fig. S6 in the supplementary material). Therefore, a prolonged interphase at the eleventh cell cycle is necessary for F-actin to accumulate at the medial end of the dorsal midline epidermis. Y-27632 treatment also abolished the accumulation of F-actin (see Fig. S6 in the supplementary material), suggesting that this phenomenon is also dependent on the Rho/ROCK pathway.

DISCUSSION

Cell division requires a large quantity of cytoskeletal elements for forming the mitotic spindle and contractile ring. Morphogenetic movement also requires a large amount of actin filament for forming filopodia/lamellipodia and microtubules for coordinated cellular movement (Rodriguez et al., 2003). It is thought that these two developmental events are incompatible, because they compete for the cytoskeletal components (Mata et al., 2000). Therefore, these two events cannot take place simultaneously and embryonic cells must regulate their timing for coordinated embryogenesis. In ascidian embryogenesis, we observed strong coordination between a single round of cell cycle progression in epidermal cells and neural tube closure. Epidermal cells prolong the G2 phase at the eleventh cell cycle to adjust the timing of the eleventh cell division so that it follows neural tube closure. This regulation is necessary because neural tube closure and the eleventh mitosis cannot take place simultaneously; epidermal cells achieve the coordination of mitosis and their morphogenetic movement by delaying the timing of mitosis. Disrupting the morphogenetic movement of the epidermis affected the sheet-to-tube morphogenesis of the neural plate, suggesting that the epidermis is necessary for the neural plate to form a tube. The contribution of the epidermis to neurulation seems to be a general feature among chordates.

During the G2 phase, dorsal midline epidermal cells elongate towards the midline to close the furrow. This cell shape change and movement, which is dependent on Rho/ROCK-mediated actin filament accumulation, could make the force that pushes the neural plate to form a tube. The morphogenetic movement and mitosis might compete against the actin filament in the epidermis during neurulation. Precocious eleventh mitosis inhibited both cell shape

Table 4. Length-width (L/W) ratio of epidermal cells during neural tube closure

	Tail dorsal midline*	Trunk dorsal midline†
Control	2.21±0.65 (*n*=67 cells)	1.69±0.56 (*n*=67 cells)
Ci-cdc25 OE	1.58±0.67 (*n*=68 cells; *P*<0.00001)‡	1.38±0.34 (*n*=78 cells; *P*=0.018)‡
Ci-cdc25 OE + Aph treated	1.98±0.50 (*n*=70 cells; *P*=0.0001)§	1.69±0.53 (*n*=75 cells; *P*=0.006)§
Y-27632 treated	1.17±0.25 (*n*=63 cells; *P*<0.00001)‡	1.25±0.25 (*n*=63 cells; *P*<0.00001)‡

*L/W ratio was measured at 8.0 hpf when tail dorsal midline epidermal cells in the control showed the highest L/W value.
†L/W ratio was measured at 8.5 hpf when trunk dorsal midline epidermal cells in the control showed the highest L/W value.
‡Statistically significant shift in the distribution of the L/W ratio compared with the control, confirmed using the Kolmogorov-Smirnov two-sample test.
§Statistically significant shift in the distribution of the L/W ratio compared with *Ci-cdc25* OE, confirmed using the Kolmogorov-Smirnov two-sample test.
Aph, aphidicolin; hpf, hours post fertilization; OE, overexpression.

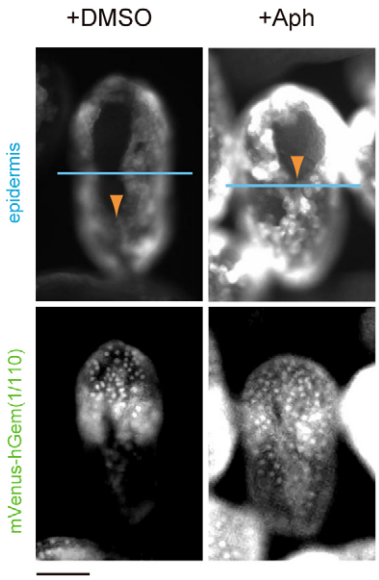

Fig. 6. Aphidicolin treatment reverses the *Ci-cdc25* overexpression effect on neural tube closure. Top row: *Ci-cdc25*-overexpressing control embryos that were treated with DMSO from 7.0 hpf (+DMSO) showed defects in neural tube closure in the tail region, whereas *Ci-cdc25*-overexpressing embryos that were treated with aphidicolin from 7.0 hpf (+Aph) completed neural tube closure in the tail region. Arrowheads represent the position of the anterior margin of the closed neural tube. Blue lines indicate the boundary between the trunk and tail. Bottom row: Fluorescence of mVenus-hGem(1/110) in the *Ci-cdc25*-overexpressing embryos. In the aphidicolin-treated embryos, some epidermal cells showed nuclear localization of mVenus-hGem(1/110), suggesting that their cell cycle progression was arrested. Scale bar: 50 μm.

change and F-actin accumulation, whereas Y-27632 treatment could not alter the timing of the cell cycle/division. Therefore, mitosis and morphogenesis in this case are not equal for the competition of actin; mitosis can overwhelm the Rho/ROCK-mediated pathway. The significance of the prolongation of the G2 phase is to make time for the Rho/ROCK-mediated pathway to accumulate F-actin and conduct cell shape change.

Epidermal cells show different mitotic timings along the A-P axis. The posterior cells divide earlier than the anterior cells. This might be another adjustment for neural tube closure, because this morphogenetic movement proceeds from posterior to anterior regions. Previous observations with a scanning electron microscope suggested that a-line epidermal cells divide slightly later than b-line cells (Nishida, 1986). This is consistent with our findings. Our observations suggest that the divisions along the A-P axis are much finer and more detailed than the broad difference between the a-line and b-line. For example, tail midline epidermal cells, which are derivatives of b4.2, start the tenth and eleventh cell divisions from the posterior side. The regulator determining the timing of cell division might work gradually along the A-P axis of the embryo. We have also shown that the epidermis can be divided into four regions with different mitotic timings in the eleventh division. Curiously, the detection of four regions with different mitotic timings coincides with the classification of epidermal cells based on clonal analysis (Pasini et al., 2006), suggesting lineage-specific determination of cell division timing. *Ci-cdc25* is probably a key regulator of the cell cycle progression of epidermal cells. The dynamic transcriptional change of this gene in the epidermis suggests that its transcriptional regulation is a crucial event for the regulation of the cell cycle. The importance of the transcriptional regulation of *Ci-cdc25* has been reported in several organisms (Edgar et al., 1994; Bissen, 1995; Wickramasinghe et al., 1995; Nogare et al., 2007) and this regulation could be common among various animals.

The orientation of mitosis is also regulated in epidermal cells during neural tube closure. At their eleventh division, epidermal cells tend to divide along the A-P axis, which is perpendicular to the orientation of neural tube closure. A plausible role of this regulation is that it provides an adjustment for the rapid elongation of the body length at this stage, which is caused by elongation of the tail. In the neurulation of chick embryos, epidermal cells divide in both a rostrocaudal and a mediolateral orientation (Sausedo et al., 1997). The former division is suggested to play a role in longitudinal lengthening, which seems to be common with *Ciona*. By contrast, the latter division might play a role in the medial expansion of the epidermis. This is in contrast with *Ciona*, in which epidermal cells do not divide during the closing of the neural tube, and cell shape change and movement towards the midline are major driving forces behind the fusion of the epidermal layer at the midline.

For the closure of the neural tube to occur, many developmental events have to be carried out in coordination. To achieve this coordination, the cell cycle of *Ciona* epidermal cells has to be regulated at the single-cell-cycle level. Such strict regulation might have been adopted because of the small cell number of ascidian embryos, in which a single round of cell division has a strong effect on overall development. It is important to elucidate the detailed mechanisms by which such cell cycle regulation is achieved. These molecular mechanisms of cell cycle regulation should be linked with those regulating neural tube closure. In vertebrates, the PCP/Wnt pathway plays crucial roles in morphogenesis, including neural tube closure (Ueno and Greene, 2003; Gong et al., 2004; Ciruna et al., 2006; Wallingford, 2006), and it is possible that similar genetic cascades regulate cell cycle progression, the orientation of cell division and morphogenesis during neural tube closure in ascidian embryos. Additionally, the description of cell cycle regulation in other cell types and morphogenetic movements in *Ciona* development is important. Previous studies have shown that neural cells of *Ciona* exhibit elongation of the cell cycle during neurulation (Nicol and Meinertzhagen, 1988a; Nicol and Meinertzhagen, 1988b). Cell cycle regulation similar to that of epidermal cells might occur in neural-fated cells; this possibility will be investigated in a future study. Fucci probes are valuable tools for observing cell cycle progression and mitosis in detail. Finally, neural tube closure is a key event in neurulation among chordates (Colas and Schoenwolf, 2001). As mentioned above, the epidermal layer contributes to proper neural tube formation in vertebrates. Epidermal cells generate the force needed to bend the neural plate via both cell division and morphogenesis (Sausedo et al., 1997). There is likely to be a mechanism that coordinates the two cellular processes in the epidermis of vertebrates. The present study indicates that fusion of the epidermis during neural tube closure occurs at the G2 phase and that cell shape change via actin regulation during this phase is a key event in *Ciona* embryos. Whether mechanisms similar to these are conserved among chordates is an interesting question.

Acknowledgements
We thank the National Bio-resource Project, Shigeki Fujiwara and all members of the Maizuru Fishery Research Station of Kyoto University and the Education and Research Center of Marine Bioresources of Tohoku University for providing us with *Ciona* adults. We are grateful to Hiroki Nishida and Patrick Lemaire for providing pBS-HTB and gateway vector set, respectively. This study was supported by Grants-in-Aid for Scientific Research from JSPS to Y.S. and N.S.

Competing interests statement
The authors declare no competing financial interests.

Supplementary material
Supplementary material for this article is available at
http://dev.biologists.org/lookup/suppl/doi:10.1242/dev.053132/-/DC1

References

Akanuma, T., Hori, S., Darras, S. and Nishida, H. (2002). Notch signaling is involved in neurogenesis in the ascidian embryos. *Dev. Genes Evol.* **212**, 459-472.
Bissen, S. T. (1995). Expression of the cell cycle control gene, *cdc25*, is constitutive in the segmental founder cells but is cell-cycle-regulated in the micromeres of leech embryos. *Development* **121**, 3035-3043.
Boutros, R., Dozier, C. and Ducommun, B. (2006). The when and wheres of CDC25 phosphatases. *Curr. Opin. Cell Biol.* **18**, 185-191.
Brouns, M. R., Matheson, S. F., Hu, K. Q., Delalle, I., Caviness, V. S., Silver, J., Bronson, R. T. and Settleman, J. (2000). The adhesion signaling molecule p190 RhoGAP is required for morphogenetic processes in neural development. *Development* **127**, 4891-4903.
Chiba, S., Satou, Y., Nishikata, T. and Satoh, N. (1998). Isolation and characterization of cDNA clones for epidermis-specific and muscle-specific genes in *Ciona savignyi* embryos. *Zool. Sci.* **15**, 239-246.
Ciruna, B., Jenny, A., Lee, D., Mlodzik, M. and Schier, A. F. (2006). Planar cell polarity signalling couples cell division and morphogenesis during neurulation. *Nature* **439**, 220-224.
Colas, J. F. and Schoenwolf, G. C. (2001). Towards a cellular and molecular understanding of neurulation. *Dev. Dyn.* **221**, 117-145.
Corbo, J. C., Erives, A., Di Gregorio, A., Chang, A. and Levine, M. (1997). Dorsoventral patterning of the vertebrate neural tube is conserved in a protochordate. *Development* **124**, 2335-2344.
Duncan, T. and Su, T. T. (2004). Embryogenesis: coordinating cell division with gastrulation. *Curr. Biol.* **14**, R305-R307.
Edgar, B. A., Lehman, D. A. and O'Farrell, P. H. (1994). Transcriptional regulation of *string* (*cdc25*): a link between developmental programming and the cell cycle. *Development* **120**, 3131-3143.
Foe, V. E. and Odell, G. M. (1989). Mitotic domains pertitoin fly embryos, reflecting early cell biological consequences of determination in progress. *Amer. Zool.* **29**, 617-652.
Fukano, T., Sawano, A., Ohba, Y., Matsuda, M. and Miyawaki, A. (2007). Differential Ras activation between caveolae/raft and non-raft microdomains. *Cell Struct. Funct.* **32**, 9-15.
Gilbert, S. F. (2006). *Developmental biology*, 8th edition. Massachusetts: Sinauer.
Gong, Y., Mo, C. and Fraser, S. E. (2004). Planar cell polarity signalling controls cell division orientation during zebrafish gastrulation. *Nature* **430**, 689-693.
Grosshans, J. and Wieschaus, E. (2000). A genetic link between morphogenesis and cell division during formation of the ventral furrow in *Drosophila*. *Cell* **101**, 523-531.
Hildebrand, J. D. and Soriano, P. (1999). Shroom, a PDZ domain-containing actin-binding protein, is required for neural tube morphogenesis in mice. *Cell* **99**, 485-497.
Hotta, K., Mitsuhara, K., Takahashi, H., Inaba, K., Oka, K., Gojobori, T. and Ikeo, K. (2007). A web-based interactive developmental table for the ascidian *Ciona intestinalis*, including 3D real-image embryo reconstructions: I. From fertilized egg to hatching larva. *Dev. Dyn.* **236**, 1790-1805.
Hozumi, A., Kawai, N., Yoshida, R., Ogura, Y., Ohta, N., Satake, H., Satoh, N. and Sasakura, Y. (2010). Efficient transposition of a single Minos transposon copy in the genome of the ascidian *Ciona intestinalis* with a transgenic line expressing transposase in eggs. *Dev. Dyn.* **239**, 1076-1088.
Ikegami, S., Taguchi, T., Ohashi, M., Oguro, M., Nagano, H. and Mano, Y. (1978). Aphidicolin prevents mitotic cell division by interfering with the activity of DNA polymerase-alpha. *Nature* **275**, 458-460.
Kawashima, T., Tokuoka, M., Awazu, S., Satoh, N. and Satou, Y. (2003). A genomewide survey of developmentally relevant genes in Ciona intestinalis. VIII. Genes for PI3K signaling and cell cycle. *Dev. Genes Evol.* **213**, 284-290.
Kipreos, E. T. (2005). C. elegans cell cycles: invariance and stem cell divisions. *Nat. Rev. Mol. Cell Biol.* **6**, 66-76.
Lehman, D. A., Patterson, B., Johnston, L. A., Balzer, T., Britton, J. S., Saint, R. and Edgar, B. A. (1999). *Cis*-regulatory elements of the mitotic regulator, *string/Cdc25*. *Development* **126**, 1793-1803.
Leise, W. F., III and Mueller, P. R. (2004). Inhibition of the cell cycle is required for convergent extension of the paraxial mesoderm during *Xenopus* neurulation. *Development* **131**, 1703-1715.
Lowery, L. A. and Sive, H. (2004). Strategies of vertebrate neurulation and a re-evaluation of teleost neural tube formation. *Mech. Dev.* **121**, 1189-1197.
Mata, J., Curado, S., Ephrussi, A. and Rørth, P. (2000). Tribbles coordinates mitosis and morphogenesis in *Drosophila* by regulating string/CDC25 proteolysis. *Cell* **101**, 511-522.
Murakami, M. S., Moody, S. A., Daar, I. O. and Morrison, D. K. (2004). Morphogenesis during *Xenopus* gastrulation requires Wee1-mediated inhibition of cell proliferation. *Development* **131**, 571-580.
Nabel-Rosen, H., Toledano-Katchalski, H., Volohonsky, G. and Volk, T. (2005). Cell divisions in the *drosophila* embryonic mesoderm are repressed via posttranscriptional regulation of *string/cdc25* by HOW. *Curr. Biol.* **15**, 295-302.
Nakayama, A., Satoh, N. and Sasakura, Y. (2005). Tissue-specific profile of DNA replication in the swimming larvae of *Ciona intestinalis*. *Zool. Sci.* **22**, 301-309.
Nicol, D. and Meinertzhagen, I. A. (1988a). Development of the central nervous system of the larva of the ascidian, *Ciona intestinalis* L. II. Neural plate morphogenesis and cell lineages during neurulation. *Dev. Biol.* **130**, 737-766.
Nicol, D. and Meinertzhagen, I. A. (1988b). Development of the central nervous system of the larva of the ascidian, *Ciona intestinalis* L. I. The early lineages of the neural plate. *Dev. Biol.* **130**, 721-736.
Nishida, H. (1986). Cell division pattern during gastrulation of the ascidian, *Halocynthia rorentzi*. *Dev. Growth Differ.* **28**, 191-201.
Nishida, H. (1987). Cell lineage analysis in ascidian embryos by intracellular injection of a tracer enzyme. III. Up to the tissue restricted stage. *Dev. Biol.* **121**, 526-541.
Nishida, H. (2005). Specification of embryonic axis and mosaic development in ascidians. *Dev. Dyn.* **233**, 1177-1193.
Nishitani, H., Lygerou, Z. and Nishimoto, T. (2004). Proteolysis of DNA replication licensing factor Cdt1 in S-phase is performed independently of geminin through its N-terminal region. *J. Biol. Chem.* **279**, 30807-30816.
Nogare, D. E., Arguello, A., Sazer, S. and Lane, M. E. (2007). Zebrafish *cdc25a* is expressed during early development and limiting for post-blastoderm cell cycle progression. *Dev. Dyn.* **236**, 3427-3435.
Pasini, A., Amiel, A., Rothbächer, U., Roure, A., Lemaire, P. and Darras, S. (2006). Formation of the ascidian epidermal sensory neurons: insights into the origin of the chordate peripheral nervous system. *PLoS Biol.* **4**, e225.
Philpott, A. and Yew, P. R. (2008). The *Xenopus* cell cycle: An overview. *Mol. Biotechnol.* **39**, 9-19.
Rodriguez, O. C., Schaefer, A. W., Mandato, C. A., Forscher, P., Bement, W. M. and Waterman-Storer, C. M. (2003). Conserved microtubule-actin interactions in cell movement and morphogenesis. *Nat. Cell Biol.* **5**, 599-609.
Roure, A., Rothbächer, U., Robin, F., Kalmar, E., Ferone, G., Lamy, C., Missero, C., Mueller, F. and Lemaire, P. (2007). A multicassette Gateway vector set for high throughput and comparative analyses in *ciona* and vertebrate embryos. *PLoS ONE* **9**, e916.
Sakaue-Sawano, A., Kurokawa, H., Morimura, T., Hanyu, A., Hama, H., Osawa, H., Kashiwagi, S., Fukami, K., Miyata, T., Miyoshi, H. et al. (2008). Visualizing spatiotemporal dynamics of multicellular cell-cycle progression. *Cell* **132**, 487-498.
Sasakura, Y., Suzuki, M. M., Hozumi, A., Inaba, K. and Satoh, N. (2010). Maternal factor-mediated epigenetic gene silencing in the ascidian *Ciona intestinalis*. *Mol. Genet. Genomics* **283**, 99-110.
Satoh, N. (1994). *Developmental Biology of Ascidians*. New York: Cambridge University Press.
Satoh, N. (2003). The ascidian tadpole larva: comparative molecular development and genomics. *Nat. Rev. Genet.* **4**, 285-295.
Sausedo, R. A., Smith, J. L. and Schoenwolf, G. C. (1997). Role of nonrandomly oriented cell division in shaping and bending of the neural plate. *J. Comp. Neurol.* **381**, 473-488.
Sugiyama, M., Sakaue-Sawano, A., Limura, T., Fukami, K., Kitaguchi, T., Kawakami, K., Okamoto, H., Higashijima, S. I. and Miyawaki, A. (2009). Illuminating cell-cycle progression in the developing zebrafish embryo. *Proc. Natl. Acad. Sci. USA* **106**, 20812-20817.
Tarallo, R. and Sordino, P. (2004). Time course of the programmed cell death in *Ciona intestinalis* in relation to mitotic activity and MAPK signaling. *Dev. Dyn.* **230**, 251-262.
Uehata, M., Ishizaki, T., Satoh, H., Ono, T., Kawahara, T., Morishita, T., Tamakawa, H., Yamagami, K., Inui, J., Maekawa, M. et al. (1997). Calcium sensitization of smooth muscle mediated by a Rho-associated protein kinase in hypertension. *Nature* **389**, 990-994.
Ueno, N. and Greene, N. D. E. (2003). Planar cell polarity genes and neural tube closure. *Birth Defects Res. C Embryo Today* **69**, 318-324.
Wallingford, J. B. (2006). Planar cell polarity, ciliogenesis and neural tube defects. *Hum. Mol. Genet.* **15**, R227-R234.
Wickramasinghe, D., Becker, S., Ernst, M. K., Resnick, J. L., Centanni, J. M., Tessarollo, L., Grabel, L. B. and Donovan, P. J. (1995). Two CDC25 homologues are differentially expressed during mouse development. *Development* **121**, 2047-2056.
Yasuo, H. and Satoh, N. (1994). An ascidian homolog of the mouse *Brachyury* (*T*) gene is expressed exclusively in notochord cells at the fate restricted stage. *Dev. Growth Differ.* **36**, 9-18.
Zhang, J., Hagopian-Donaldson, S., Serbedzija, G., Elsemore, J., Plehn-Dujowich, D., McMahon, A. P. and Flavell, R. A. and Williams, T. (1996). Neural tube, skeletal and body wall defects in mice lacking transcription factor AP-2. *Nature* **381**, 238-241.